7th Australasian Hydraulics and
Fluid Mechanics Conference,
Brisbane, 18-22 August, 1980

The Evaporation of Small Mist Droplets from a Vertical Plate Using a Two-Dimensional Air Jet

R.R. HORSLEY

Senior Lecturer, Department of Mechanical and Production Engineering, Royal Melbourne Institute of Technology

SUMMARY A theoretical and experimental method is presented to predict the evaporation rate of mist droplets from a vertical glass plate using a hot two-dimensional air jet. The theoretical model defines an effective evaporating temperature in the boundary layer and takes into account variable wall heat fluxes and variable positions on the plate. The model also develops a similar expression for the effective partial pressure of the water vapour in the boundary layer which is needed to accurately predict mass transfer rates from the plate. A novel experimental technique has also been developed to measure the change in mist droplet thickness as a function of time. A light source beamed parallel light through the mist and an extremely sensitive photocell was used to measure the change in intensity of light as the mist dried. A large amount of data was collected and has been correlated. A non-dimensional transient mass transfer number was determined which enables the prediction of the drying phenomena for the whole plate. An important parameter namely the coverage factor, relates the experimental results to those theoretically derived and gives reliable predictions.

1 INTRODUCTION

A practical example of wall jet flows is the demisting of motor vehicle windscreens, where essentially two dimensional hot air jets evaporate the mist formed on the windscreen.

2 THEORETICAL MODEL

2.1 The Effective Temperature

In most previous work, the wall jet has discharged into a moving mainstream due to its relevance to film cooling. Jacob et al (1950, and Seban et al (1962) have obtained some correlations of the heat transfer coefficients for a two-dimensional wall jet in stagnant surroundings. They found that the heat transfer data could be correlated by using t_{max} as the effective temperature in the boundary layer. Thus, the suggestion of Jacob et al (1950) and Patel (1971), implies that the effective temperature is not affected by the magnitude of the jet temperature. This is obviously untrue and, therefore, their correlation equation does not apply for the case where t_j is less than t_o. Spalding (1963) has postulated formulae to predict mass transfer rates and some of these results have been used to predict the demisting rates. The model used in this paper is based on the Reynolds Flow Model.

In order to determine the local heat transfer coefficient on the plate, it is necessary to find the correct value of the effective temperature at that position. In order to determine the heat transfer behaviour of the wall jet the choice of the correct value of t_e is essential. The logical choice would be to choose the maximum temperature t_{max} within the jet boundary layer as the effective temperature. This argument follows logically as long as t_j is greater than t_o, but it becomes meaningless when t_j is less than t_o. The explanation being that when t_j is less than t_o, t_{max} is always the same as t_o, which is implying that the effective temperature is independent of the jet temperature.

The best way of assessing the wall heat flux would be to consider that this wall heat flux would increase if $(t_j - t_s)$ or $t_o - t_s)$ increase, even if the Reynolds number remains unaltered. The assumption is implying that $(t_e - t_s)$ is a linear function of $(t_j - t_s)$ and $(t_o - t_s)$ to give

$$(t_e - t_s) = a(t_o - t_s) + b(t_j - t_s) \qquad (1)$$

where a and b are only dependent on geometry and Reynolds number.

For any position on the plate, and assuming Pr is essentially invariant

$$Nu = hL/k = \frac{\dot{q}''_w L}{k(t_e - t_s)} \qquad (2)$$

Because L is a constant for any position on the plate, equation (2) becomes

$$\frac{\dot{q}''_w}{k(t_e - t_s)} \simeq \text{constant} \qquad (3)$$

Equation (3) can now be written in terms of the effective temperature

$$\frac{\dot{q}''_{w_1}}{k_1\,[a_1(t_o - t_s)_1 + b_1(t_j - t_s)_1]} = \cdots\cdots$$

$$\frac{\dot{q}''_{w_n}}{k_n\,[a_n(t_o - t_s)_n + b_n(t_j - t_s)_n]} \qquad (4)$$

where n is the number of tests in any one position.

Now at any position on the plate, the properties of the fluid can be determined at a chosen film temperature. At two different positions a pair of simultaneous equations is then obtained from equation (4) which contains only two unknowns, a and b, letting η equal a/b and assuming equation (1) is correct then η should be constant at a particular position on the plate regardless of the values of t_o and t_j, provided that the conditions listed above remain the same. This results in

$$a = \frac{\eta}{1+\eta} \text{ and } b = \frac{1}{1+\eta}$$

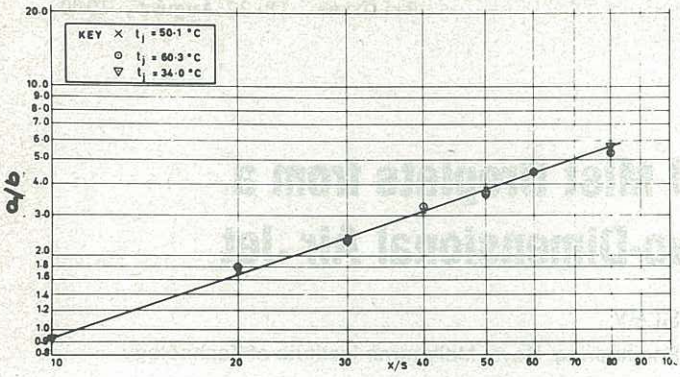

Figure 1 Variation of η with non-dimensional plate length

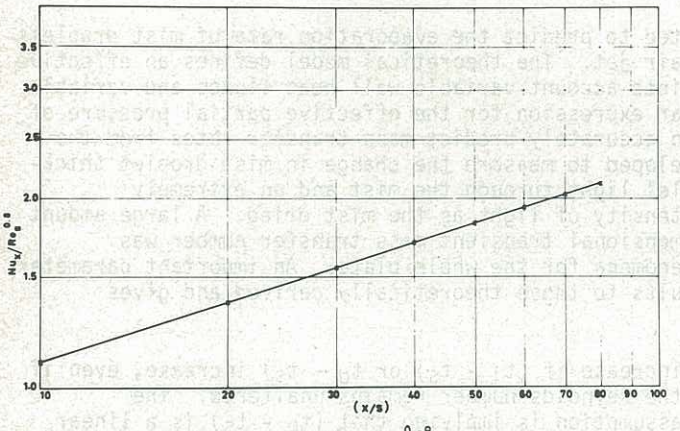

Figure 2 Variation of $Nu_x/Re_s^{0.8}$ with non-dimensional plate length

and hence equation (1) can now be written as

$$t_e = \frac{1}{1+\eta}(t_j + \eta t_o) \quad \text{or} \quad \eta = \frac{t_j - t_e}{t_e - t_o} \qquad (5),(6)$$

An iteration process is then required as the initial t_e evaluated was based on a k at a chosen film temperature. k is then recalculated based on this value of t_e and new values of a and b are found.

It was found by this iteration process that the values of η at any particular location did not vary much and by using the theory of least squares, it was found that the standard deviation around the values of η was within ±3%. The following correlation was then found for η (see Fig. 1)

$$\eta = 0.127\ (\frac{x}{s})^{0.865} \qquad (7)$$

Using these values of η the values of t_e and hence h were calculated. A local Nusselt number was then established. Because of the apparent dependence of Nu_x on the location, values of log $(Nu_x/Re_s^{0.8})$ where plotted against log (x/s)(Fig. 3) to obtain

$$Nu_x = 0.532\ Re_s^{0.8}\ (\frac{x}{s})^{0.316} \qquad (8)$$

and including the Prandtl Number to give

$$Nu_s = 0.532\ Re_s^{0.8}\ Pr^{0.33}\ (\frac{x}{s})^{-0.684} \qquad (9)$$

2.2 Transient Heat Transfer to the Glass Plate

It is now necessary to determine the way in which the glass surface temperatures change with time. The jet flow becomes fully established in respect to its velocity and temperature profiles, in a very short time, but the temperature distribution within the plate takes a much longer time to reach steady state conditions. Assuming the heat flow through the glass to be essentially one-dimensional heat conduction, the following equation applies

$$\frac{\partial^2 t}{\partial y^2} \quad \frac{1}{\alpha}\frac{\partial t}{\partial \tau} \qquad (10)$$

At any time chosen, the value of the heat transfer coefficient can be determined from the previously derived Nusselt number equation (8). Using a simple finite difference analysis to solve equation (10), the temperature distribution in the plate can be found.

2.3 Convective Mass Transfer

In the evaporation of moisture from a flat vertical glass plate the problem to be solved involves the mass transfer between a water film consisting of droplets on a surface and a wall jet. For convective heat transfer from a wall, equation (11) shows that

$$\dot{q}''_w = -k(\frac{\partial t}{\partial y})_s = h(t_e - t_s) \qquad (11)$$

Similarly, for diffusion of a substance from the surface to the main stream flow, the mass transfer

$$\dot{m}'' = \frac{D_i}{R_i T_s}(\frac{\partial p_i}{\partial y})_s. \qquad (12)$$

Spalding defines a flux g_{ht} as

$$\frac{g}{g_{ht}} = h/c_p \qquad (13)$$

For the mass transfer between a water film on a surface and an airstream, Spalding defines a driving force B as

$$B = \frac{m_e - m_s}{m_s - 1} \qquad (14)$$

The mass transfer rate is then given by

$$\dot{m}'' = g \log_e (1 + B) \qquad (15)$$

where g is related to g_{ht} by

$$\frac{g}{g_{ht}} = Le^{(1-n)} \qquad (15)$$

In order to determine the value m_e the partical pressure of the water vapour at this effective temperature needs to be determined. A similar analysis as to that for the effective temperature has been used. It is reasonable to expect that the expressed for t_e (equation 5) could also be used to give an effective partial pressure p_e in terms of p_j and p_o, thus

$$p_e = (p_j + \eta p_o)/(1 + \eta) \qquad (17)$$

The mass transfer is then calculated using equation (15).

3 EXPERIMENTAL MODEL

3.1 A glass plate approximately the size of a motor vehicle windscreen together with a two-dimensional jet from which air could be delivered at known temperatures and humidities was fitted into the side of an environmental chamber. The temperature in the chamber could be controlled so that the glass temperature at the beginning of each test could remain at a fixed value. A steam generator was built to generate steam. This steam was ducted away in a hose and sprayed onto the cold glass surface. The coverage of moisture on the surface was calibrated by weighing a sample of the glass specimen a number of times to ensure an even mist distribution (Horsley, 1976). To determine the thickness of the water droplets the method used was to focus on the top of each droplet with very high magnification (1094) and then to focus on the top

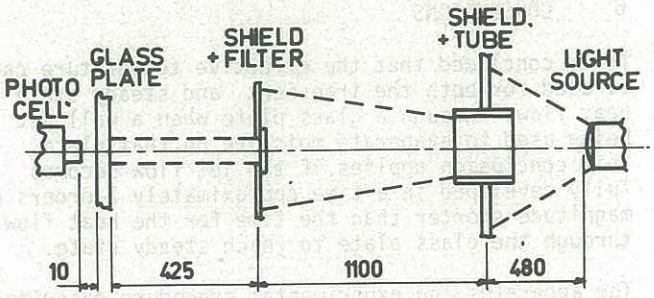

Figure 3 Schematic of Optical Measurement Rig

of the glass plate. The distance moved by the object lens could be read directly from the microscope to 0.0002 mm and this then would give the thickness of the droplet. For calibration purposes, a piece of windscreen glass was epoxied onto a small stand which stood on a pan on an accurate Sartorious mass balance. The calibration rig was placed in the environmental research chamber and the temperature of this room was kept at a value just above the dew point of the air surrounding the calibration specimen. This mass could be read to an accuracy of 10^{-4} gr. A photocell was positioned in the correct horizontal plane and placed 10 mm from the glass specimen (see Fig. 3). This distance remained constant during the whole calibration procedure and during all the evaporation tests. A light source was positioned in the same horizontal plane and the output voltage was recorded on the chart recorder. One side of the glass specimen, the side opposite to the photocell, was sprayed in the usual manner with steam from the steam generator. The same procedure was then adopted for the full demisting rig.

3.2 Measurement Techniques

The method of using light to measure change in moisture thickness appears to be advantageous over other methods as no probes interfere with the airflow over the misted surface. The method of applying the mist uniformly was satisfactory and the calibration technique relating mist thickness to light intensity is considered successful (Horsley, 1976). The point to be stressed is, that while the droplets are drying, their diameter becomes smaller so that dry gaps appear between each droplet. This means that the effective area from which the average mass transfer is calculated is reduced with time. This leads to the introduction of a term called the coverage factor. Fig. 4 shows this coverage factor which is a relationship between the area still covered with moisture as a function of time.

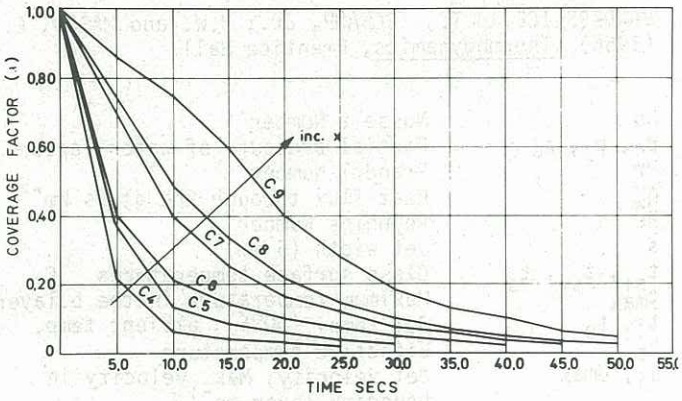

Figure 4 Area of Glass Plate covered with Mist

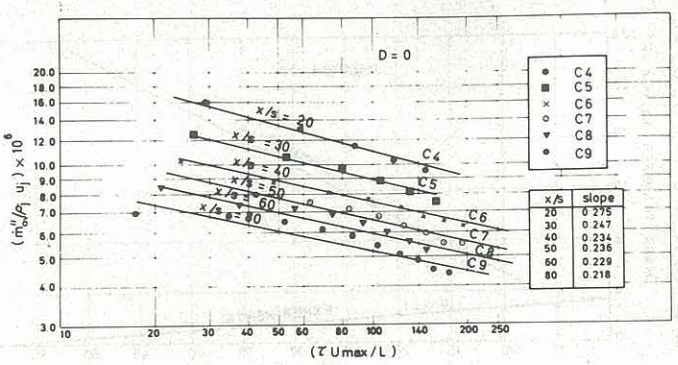

Figure 5 Experimental Mass Transfer

3.3 Experimental Correlations

Due to the large amount of experimental data recorded, it was necessary to correlate the results. Initially, using dimensional analysis, it was found that the experimental mass transfer could be expressed as

$$\dot{m}''_{exp}/\rho_j u_j = f[\frac{\tau U_{max}}{L}; \frac{x}{s}] \qquad (18)$$

Fig. 6 shows a plot of non-dimensional mass transfer against non-dimensional time in varying positions on the plate. By the use of a first-order least squares fit on these experimental results, the slope for each position on the plate was found. These slopes are tabulated on fig. 5. By taking the average of the slopes, i.e. 0.239, a correlation was found in the form

$$(\frac{\dot{m}''_{av}}{\rho_j u_j})(\frac{\tau U_{max}}{L})^{0.239} = \text{constant} \qquad (19)$$

where the constant is a function of x/s, the non-dimensional parameter Ho is then defined as

$$Ho = (\frac{\dot{m}''_{av}}{\rho_j u_j})(\frac{\tau U_{max}}{L})^{0.239} \qquad (20)$$

and fig. 6 shows a curve of Ho plotted against x/s to give the final correlation

$$Ho = 15.9 \times 10^{-5}(x/s)^{0.53} \qquad (21)$$

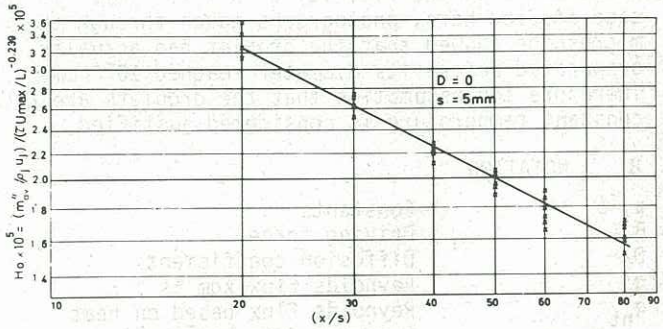

Figure 6 Experimental Mass Transfer Correlation

Bearing in mind that the calibration technique for determining the experimental mass transfer using the photocell method has an accuracy of approximately ±10%, the scatter in the correlation equation can be considered to be quite reasonable and lies within the calibration band of ±10%.

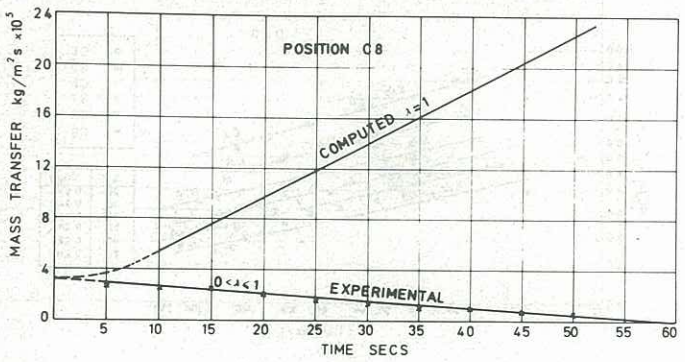

Figure 7 Comparison between Numerical and Experimental Mass Transfer

5 RELATIONSHIP BETWEEN THEORETICAL AND EXPERIMENTAL RESULTS

In comparing the mass transfer rates from the windscreen obtained experimentally with those determined numerically, it must be remembered that the theoretical model was derived assuming that the moisture did not evaporate to leave gaps between discrete droplets. Therefore, the coverage factor is the parameter which relates the two methods to determine whether the theoretical model is accurately predicting what is happening in the real situation. Fig. 7 shows the relationship between the computed results, where the coverage factor is assumed to be to 1, and the experimental results, where the coverage factor varies between 0 and 1 for two positions on the plate. It can be seen from these results that the distance between the two curves should be a measure of the coverage factor and should be the same value as that obtained by taking photographs of the mist whilst it was drying. This, in fact, is the case and that the ratio of the experimental mass transfer rates from the plate to the theoretically computed mass transfer rates gives the coverage factor. In determining the theoretical mass transfer, it was assumed that the mist droplets were so small that their thermal capacity was negligible and that they evaporated at a constant temperature equal to the temperature of the surface of the glass (t_{s_1}). Vanderslice et al (1966) points out that the vapour pressure of small droplets is appreciately increased if the droplet diameter is made small enough, if the vapour pressure increases and the temperature of the droplet increases. This increase in temperature, however, is only noticeable when the droplet diameter is in the vicinity of 3×10^{-6} mm. In the case studied here, photographs taken through the microscope showed that the droplet had actually evaporated before its diameter reached 10^{-5} mm. Therefore the assumption that the droplets are at a constant temperature is considered justified.

8 NOTATION

a, b	Constants
B	Driving force
D_1	Diffusion coefficient
g	Reynolds Flux $kgm^{-2}s^{-1}$
g_{ht}	Reynolds Flux based on heat transfer data $kgm^{-2}\ s^{-1}$
h	Heat transfer coefficient $Wm^{-2}{}^{o}C^{-1}$
k	Thermal conductivity $Wm^{-1}K^{-1}$
L	Length m
Le	Lewis number
m_e, m_s	Mass fraction of water vapour at t_e and t_{s1}
$\dot{m}''$	Mass transfer $kgm^{-2}s^{-1}$
Nu	Nusselt Number
Pe, Pj, Po	Partial pressure of water vapour
Pr	Prandtl Number
q''_w	Heat flux through the glass Wm^{-2}
Re	Reynolds Number
s	Jet width (5 mm)
t_{s1}, t_{s2}, t_s	Glass surface temperatures ^{o}C
t_{max}	Maximum temperature in the b.layer
t_j, t_o	Jet temp. ($50^{o}C$); ambient temp.
t_e	Effective temperature
u_j, Umax	Jet velocity; Max. velocity in boundary layer ms^{-1}
α	Thermal diffusivity m^2s^{-1}
ρ_j; τ	Jet density kgm^{-3}; Time s

6 CONCLUSIONS

It is concluded that the effective temperature can be used for both the transient and steady state heat flows through a glass plate when a wall jet is being used to evaporate moisture on that plate. This conclusion applies if the jet flow becomes fully developed in a time approximately 2 orders of magnitude shorter than the time for the heat flow through the glass plate to reach steady state.

The apparatus and experimental procedure described to determine the experimental mass transfer proved quite successful and yields reproducable and, it is hoped, accurate results. The novel photocell technique used to determine the transient mist evaporation has been calibrated and has proved to be successful and has allowed a new correlation equation to be determined for the experimental mass transfer. An expression for the effective partial pressure was developed based on the analogy between heat and mass transfer, and is of the same form as the expression for the effective temperature. The effective partial pressure has been used to determine the driving force that is necessary to calculate the theoretical mass transfer. It is concluded that the assumption, of the mist film being continuous, is adequate. This assumption allowed Spalding's technique to be used to predict the theoretical mass transfer rates from the glass plate. The fact that the mist film was not continuous was alllowed for in the use of the coverage factor and the use of this parameter shows that both the theoretical and experimental models predict the rate at which the moisture evaporates.

7 REFERENCES

HORSLEY, R.R. (1976) An experimental and theoretical analysis of transient demisting phenomena as applied to wall jet flows. Thesis (PhD) Univ. of the Witwatersrand.

JACOB, M., Rose, R.L. and SPIELMANN, M. (1950) Heat transfer from an air jet to a plane plate with entrainment of water vapour from the environment. Trans. ASME, Vol. 72, p. 859.

PATEL, R.P. (1971) Turbulent jets and wall jets in uniform streaming flow. Aeronautical Quarterly, Vol. 22, p. 311.

SEBAN, R.A. and BACK, L.H. (1962) Velocity and temperature profiles in turbulent boundary layers with tangential injection. J. of Heat Transfer, Trans. ASME (Series C) Vol. 84, No. 1, p. 45.

SPALDING, D.B. (1963) Convective Mass Transfer, Edward Arnold.

VANDERSLICE, J.T., SCHAMP, Jr., H.W. and MASON, C.E. (1966) Thermodynamics, Prentice Hall.